

# **Design and Mathematical Modelling of C<sub>3</sub>H<sub>8</sub> Emission from Gas Cylinder Holding in a Liquefied Phase of Gas**

**Engr. Unyime Enobong Okure**

*Department of Chemical Engineering  
Niger Delta University, Bayelsa, Nigeria*

**Engr. Nnadikwe Johnson**

*Department of Chemical Engineering  
Imo state Polytechnic, Owerri Nigeria*

**Engr. Ibe Raymond Obinna**

*Department of Chemical Engineering  
Imo state Polytechnic, Owerri Nigeria*

**Khama Rieborue Emmanuel**

*Department Of Petroleum And Gas Engineering  
Nigeria Maritime University, Okerenkoko, Delta State*

**Engr. Benedict Okon Edenseting**

*University of Uyo, Uyo  
Nigeria*

## **ABSTRACT**

You'll see boiling, heat transfer from the atmosphere, heat exchange between the tank's interior and its liquefied gas in addition to mass loss after gas-phase discharge from a tank holding that gas. The goal of this study is to simulate the thermal reaction of a tank containing liquid gas during the emission of a vapor phase jet. The heat transfer between the tank's shell and the air, as well as the liquid phase, vapor phase, and mass balance, is considered. Pressure within the tank is predicted, as well as temperature of the tank's shell, temperature of the liquid and vapor phases, as well as mass loss from the tank, using the approved model. A comparison was made between the theoretical model's predictions and the actual outcomes of the tests. Ten kilograms of propane were stored in a typical residential LPG tank for the experiment's purpose (27 dm<sup>3</sup> volume). For example, temperature and pressure may be properly predicted before vapor phase emission occurs from a liquid gas tank using the model shown here.

-----  
Date of Submission: 10-07-2022

Date of Acceptance: 25-07-2022  
-----

## **1 Introduction**

It is necessary to construct emergency scenarios and risk assessments for the storage and transport of liquid gases in pressure tanks. Liquid media under pressure tanks may be found in refineries, energy, and transportation sectors. It's a revolutionary approach to employing propane-butane as a natural gas alternative in tanks and portable cylinders at home.

Many scholars have studied the events that take place in a tank when the safety valve is opened, and it's a complicated issue that requires consideration of a wide range of factors. This happens when the liquid boils quickly and the safety valve is quickly opened, or if the tank's top half has been damaged. Because the boiling point is so low, even with two-phase emission, this process is very demanding. The mass and energy balance of the liquid-vapor-tank-environment system represents the evaporation of the vapor phase from the tank. Steam condensation and freezing, as well as mass exchange throughout the boiling phase and emission via the exit, are the most challenging aspects of heat exchange with the environment.

**2 Experimentation and modeling**  
**2.1. Model**

During an emergency discharge, the thermodynamic properties of the propane jet outflow from the tank change. Temperatures in both the gas and liquid phases are included in the model, as is mass in the gas phase and mass in the liquid phase, as well as temperatures in the top and lower portions of the tank walls that come into contact with the gas phase and liquid phase, respectively. When the jet is outflowing and igniting, the model analyses the variations in these parameters. Isentropic-adiabatic discharge takes place via a fixed-diameter outlet. The algorithm takes into account both throttled and unthrottled flow depending on the tank's pressure. Mathematical computing environment Matlab was used to do the computations.

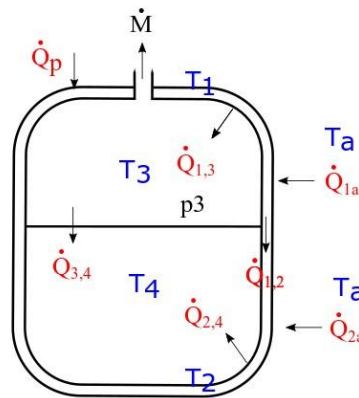


**Fig. 1.**A propane tank and surrounding

Conditions of exclusion:

1. Initial equilibrium between the liquid and gas phases occurs.
2. There is also a state of equilibrium inside the tank-environment system, which means that the starting temperatures of the liquid phase, gas phase, and tank
3. The temperature in the room remains steady at 68.3 degrees Fahrenheit.
4. The tank's walls are considered to be infinitely thin shells in terms of heat flux (with the flow of heat the thickness of the tank is not taken into account),
5. In calculations, the tank is represented as a single homogeneous cylinder.
6. It has been shown that the bottom and top components of the tank interact with the liquid and gas phases via an imagined line traced across its shell.
7. Seven. The temperature of the tank's liquid, gas, and shell components are all the same across its whole volume.
8. In this model, all of the coefficients are viewed as constants, regardless of whether or not the thermodynamic parameters themselves vary.
9. As a result of this, all of the following values are treated as time-dependent variables: heat exchange coefficients, mass streams (outflow and evaporation), liquid and gas phase density, both phase heights, heat exchange surfaces, heat flux from the environment, heat flux delivered from a fire, heat flux of liquid phase vaporization, and pressure in the tank.

Using the equations below, we may track the evolution of various parameters over time:

$$\left\{ \begin{array}{l} Q_1 = \dot{Q}_{1a}t - \dot{Q}_{1,3}t - \dot{Q}_{1,2}t + \dot{Q}_p t \\ Q_2 = \dot{Q}_{2a}t + \dot{Q}_{1,2}t - \dot{Q}_{2,4}t \\ Q_3 = \dot{Q}_{1,3}t - \dot{Q}_{3,4}t - \dot{Q}_{str}t \\ Q_4 = \dot{Q}_{2,4}t + \dot{Q}_{3,4}t - \dot{Q}_{lg}t \\ m_3 = m_{30} - \dot{M}_{str}t + \dot{M}_{lg}t \\ m_4 = m_{40} - \dot{M}_{lg}t \end{array} \right. \quad (1)$$

of which the following is an example:

$$\left\{ \begin{array}{l} \frac{dT_1}{dt} = \frac{h_{1a}A_{1a}(T_a - T_1)t - h_{1,3}A_{1,3}(T_1 - T_2)t - h_{st}A_{st}(T_1 - T_2)t + \dot{Q}_p t}{m_1 c_{st}} \\ \frac{dT_2}{dt} = \frac{h_{2a}A_{2a}(T_a - T_2)t + h_{st}A_{st}(T_1 - T_2)t - h_{2,4}A_{2,4}(T_2 - T_4)t}{m_2 c_{st}} \\ \frac{dT_3}{dt} = \frac{h_{1,3}A_{1,3}(T_1 - T_3)t - h_{2,4}A_{2,4}(T_2 - T_4)t - \dot{Q}_{str} t}{m_3 c_3} \\ \frac{dT_4}{dt} = \frac{h_{2,4}A_{2,4}(T_2 - T_4)t + h_{2,4}A_{2,4}(T_3 - T_4)t - \dot{Q}_{lg} t}{m_4 c_4} \\ \frac{dm_3}{dt} = -\dot{M}_{str} t + \dot{M}_{lg} t \\ \frac{dm_4}{dt} = -\dot{M}_{lg} t \end{array} \right. \quad (2)$$

The formula [27], which includes the throttled outflow criteria, was used to compute the mass flow rate (mstr):

$$p_3 \geq p_a \left( \frac{\gamma+1}{2} \right)^{\frac{\gamma}{\gamma-1}} \quad (3)$$

Using the following equation, the throttled flow was determined:

$$\dot{M}_{str} = A_h p_3 \left[ \frac{yM}{RT_3} \left( \frac{2}{\gamma+1} \right)^{\frac{\gamma+1}{2}} \right]^{\frac{1}{2}} \quad (4)$$

The unthrottled outflow equation is:

$$\dot{M}_{str} = A_h \sqrt{2\rho_3 p_3 \left( \frac{y}{y-1} \right) \left[ \left( \frac{p_a}{p_3} \right)^{\frac{2}{y}} - \left( \frac{p_a}{p_3} \right)^{\frac{y+1}{y}} \right]} \quad (5)$$

The formula [24] describes the jet fire's heat flux:

$$\dot{Q}_p = \frac{A_{24} \eta \tau_a \dot{M}_{str} H_{comb}}{4\pi x^2} \quad (6)$$

In order to evaporate a boiling liquid, the heat flow required is calculated as follows (21):

$$\dot{Q}_{lg} = A_{34} \mu_4 h_{lg} \left[ \frac{(\rho_4 - \rho_3) g z}{\sigma} \right]^{0.5} \left[ \frac{c_{p4}(T_2 - T_{sat})}{c_{sf} h_{lg} Pr_l^n} \right]^3 \quad (7)$$

$$\dot{M}_{lg} = \frac{\dot{Q}_{lg}}{h_{lg}} \quad (8)$$

Evaporation's mass flow:

Formulas for calculating the starting mass of gaseous and liquid phases were employed as follows:

$$\left\{ \begin{array}{l} m_{30} + m_{40} = m_{netto} \\ \frac{m_{30}}{\rho_{30}} + \frac{m_{40}}{\rho_{40}} = \pi r^2 H_{zb} \end{array} \right. \quad (9)$$

The liquid-vapor balance was calculated with the use of the Peng-Robinson equation [28], as follows:

$$p = \frac{RT}{V-b} - \frac{a\alpha(T)}{V(V+b)+b(V-b)} \quad (10)$$

Equations [26] were used to compute the heat exchange coefficients between the surrounding environment and the top and bottom tank sections:

$$h_{1a} = 1,31(T_1 - T_a)^{\frac{1}{3}} \quad (11)$$

$$h_{2a} = 1,31(T_2 - T_a)^{\frac{1}{3}} \quad (12)$$

In order to compute the heat transfer coefficient between tank wall and gas phase, we used the following equation:

$$h_{13} = \frac{k_2 C R a_2^{\frac{1}{3}}}{H_g} \quad (13)$$

where:

$$R a_2 = \frac{g z \beta_2 (T_1 - T_2) H_g^3}{\alpha_3 \nu_2} \quad (14)$$

gas thermal expansion coefficient:

$$\beta_3 = \frac{2}{T_1 + T_3} \quad (15)$$

The subsequent equation was used to compute the tank wall-to-liquid heat exchange coefficient:

$$h_{2,4} = \frac{k_4 C R a_4^{\frac{1}{3}}}{H_r} \quad (16)$$

The wall's heat transfer coefficient [27]:

$$h_{st} = \frac{k_{st}}{\sqrt{k_{st} g \left( \frac{1}{\sqrt{h_{1a} + h_{13}}} + \frac{1}{\sqrt{h_{2a} + h_{24}}} \right)}} \quad (17)$$

Nusseltel, Jakob, and Prandtl [27] was used to calculate the liquid-to-gas heat transfer coefficient.

$$h_{3,4} = \frac{k_4 \cdot J a^2}{d \cdot C_{mb}^2 \cdot Pr^l} \quad (18)$$

## 2.2. Experiments

Experiments utilized 27 dm<sup>3</sup> water and 10 kilogram propane cylinders. A valve-equipped head was created to introduce a thermocouple and pressure sensor into the cylinder. During the tests, the liquid phase, vapor phase, tank wall, pressure, system mass, and outside temperature were observed. Figure 2 depicts current visible and infrared studies.

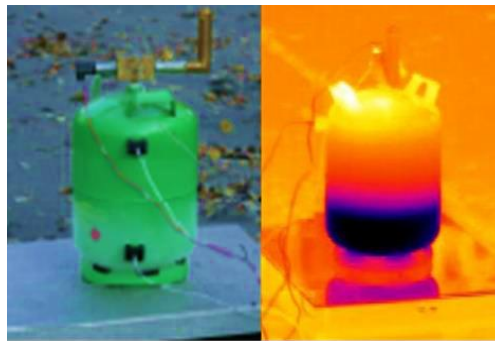


Fig. 2. Research stand – VIS and IR image.

## 3 Results and discussion

During the system's balanced gas outflow, the tank pressure dropped. As the pressure lowers, the liquid boils because the saturation temperature is lower. Difference between liquid phase temperature and saturation temperature at stipulated pressure determines boiling intensity. Evaporating liquid absorbs system heat. The mechanism absorbs less heat than is needed to evaporate liquid. During jet outflow, tank temperature decreases in both phases and areas. Figures 3-6 compare model-generated and experimental temperature variations. Results are displayed for 6, 5, 4, and 2 mm outlet sizes.

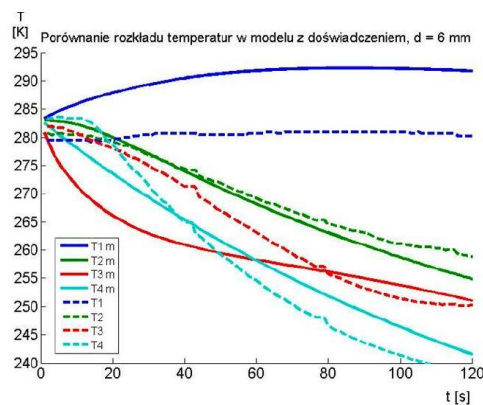


Fig. 3. Model and experimental temperature variations for 6-mm outflow.

The jet firing only raises the temperature of the tank's top half (T1). This is the impact of the flame's thermal radiation (750 W beginning stream) when the outflow is pointed vertically upwards. The lowest liquid phase temperature (T4) shows that evaporating it requires a lot of heat. Lower tank temperature (T2) drops as liquid temperature does. T2 falls slower than T4. The liquid absorbs heat from the tank's bottom. In gas phase, temperature varies (T3). Its temperature drops faster than the liquid phase at first, then becomes gentler, and subsequently the liquid phase's temperature drops significantly. Gas phase heat discharge causes the early phase's quick drop. As tank pressure drops, the outflow slows.

Temperature data during jet fire tests with a 6 mm diameter at 280-285K confirm the model's temperature predictions. The top tank (T1) temperature rose by 10 degrees Celsius, which was not observed. The estimate assumes the flame's form doesn't vary and wind isn't an issue. The simulation's lowest tank temperature (T2) matches the real-world temperature. The model's liquid phase temperature (T4) matches the practical test's. The model's T4 temperature lowers continuously over time, although the first minute's reduction is more noticeable than later minutes. The gas phase temperature (T3) converged in simulation and real data, although diverging in the first phase. Simulated model computations took 120 seconds. The model doesn't incorporate film boiling. Film boiling reduces evaporation heat flow. Once a sufficient temperature difference is reached between the liquid and saturation temperature, the liquid phase temperature decrease, T1, T2, and gas phase temperature increase slow down.

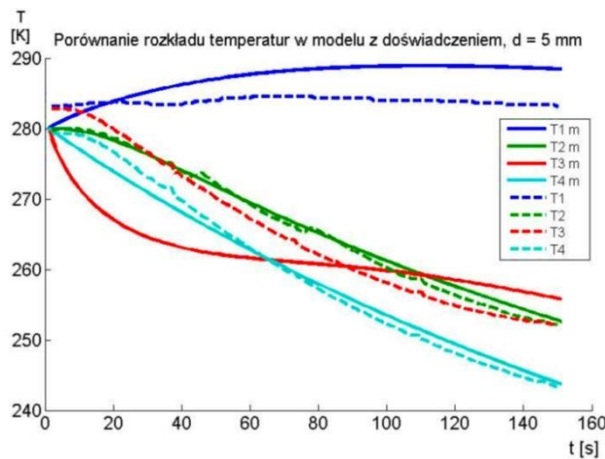


Fig. 4. Model and experimental temperature variations for 5 mm outflow.

Experimental temperatures for 5 mm outflow and 280-285K ambient support the model's temperature changes. For this outflow, the model's findings are more accurate. T4 and T2 are essentially identical throughout the simulation. The estimated gas phase temperature (T3) deviates from real data for a brief period, but the overall trend is maintained and the final simulation phase temperatures are identical. Figure 3 and the model temperature of the top half of the tank (T1) both rise, but T1 stays relatively constant.

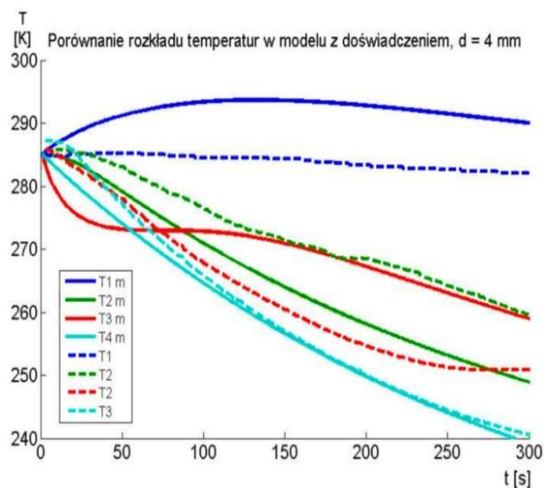


Fig. 5. Model and experimental temperature variations for 4-mm outflow.

When Matlab results are compared to experimental data for a 4 mm outflow, liquid phase temperatures (T4) are quite close throughout the simulation. T2 (lower tank) has a different temperature than calculated. Humidity or wind speed might cause the changes. The highest tank temperature (T1) remains the same. Calculations revealed a higher temperature. Gas phase temperature estimates and actual results vary substantially (T3).

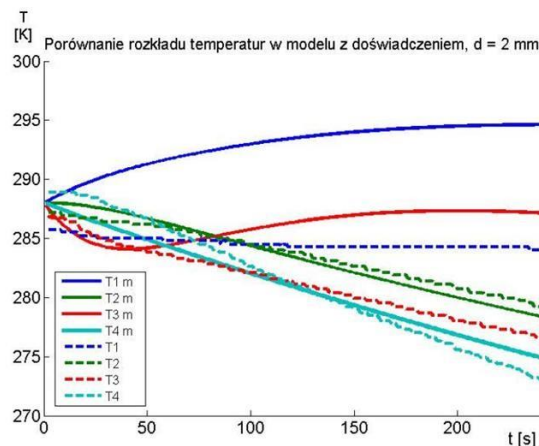


Fig. 6. Model and experimental temperature variations for 2-mm outflow.

In a 2 mm outflow, the liquid phase temperature (T4) and lower tank temperature (T2) are equivalent to experimental results. The gas phase (T3) and the tank's top half were at different temperatures (T1). The estimated temperature T1 in the final phase is around 10 K higher than the actual temperature, which is consistent with earlier measurements. Although the simulation's gas phase temperature (T3) is 10 K higher than the experiment's, the difference is significant at bigger diameters. In the event of a 2 mm outflow, the jet was substantially smaller than in prior study, resulting in less heat being absorbed for liquid evaporation. T4 and T2 temperatures dropped more slowly than before. The simulation created an exaggerated rise in T3 due to an increase in T1. Model findings are close to experimental data for liquid phase temperature change (T4). After a few seconds of steady temperature, the drop is rapid at first and slower thereafter. T2 looks to be the same as T1 (T1). Gas phase temperatures are more variable (T3). The downward trend is maintained, and the final phase temperature difference is minor, but the model's temperature decline is much quicker in the early phase. The model and experiment diverge at the highest tank temperature (T1). The model's temperature increases by fewer than 10 degrees Celsius, while the experiment's stays stable. The model assumes wind speed and a steady, defined flame. Fire heat flux was lower than predicted.

#### 4 Conclusions

The first conclusion is based on the jet outflow temperature without ignite after comparing computer model results to experimental investigation data. Under these circumstances, liquid, gas, upper tank shell, and lower tank shell temperatures all drop. The liquid phase cools the most, whereas the top tank cools the least. The liquid's temperature drops due to the heat needed to evaporate it. The bottom tank half and gas phase temperature are greatly lowered. As time passes, the evaporation stream decreases, requiring less heat. Liquid phase and lower tank temperature stay steady, but gas phase temperature increases. Evaporation heat affects system temperature distribution the most. First impressions of jet fire are that the situation should alter substantially compared to jet outflow without igniting. Not so in practice. Liquid, gas, and tank bottom temperatures are all falling. The top tank's temperature is constant and doesn't increase. Only flame heat affects the tank's top.

The jet outflow model uses thermodynamic concepts and criteria equations to describe jet fire behavior. According to Matlab simulations, liquid temperature decreases greatest during jet outflow. Lower tank and gas phase temperatures fell less. Upper tank temperature drops somewhat. During a jet fire, the liquid's temperature changes steadily while the tank's temperature stays constant. The gas phase temperature declines quicker than the tank's top, contrary to experiments. Assuming flame stability and shape consistency throughout the simulation, plus the lack of ambient conditions, raises the tank's temperature. After performing models for jet burns at the outflow with varying diameters, it was shown that temperature drops faster as the diameter widens. The liquid phase has the biggest temperature changes, whereas the top tank has the least. The ambient temperature has a minimal influence on the pace of temperature changes, but the beginning temperatures of various phases and areas of the tank are greater. The suggested calculating model simulates fire situations.

According to the models and tests, the patterns in tank temperature changes and mass loss are true. The liquid phase and lower tank temperature change courses are similar to real-world outcomes. During simulation, the top part of the tank is always hotter than the lower half. The discrepancy stems from the assumption that the flame is steady. Underappreciated atmospheric factors include wind speed. These assumptions effect gas temperature variations.

### Acknowledgement

The authors would like to acknowledge the centre for energy resources and refining technology at Imo State University, Owerri, Nigeria for their technical support, especially providing access to their own software application.

### References

- [1]. M. Bi, J. Ren, B. Zhao, W. Che, *Journal of Hazardous Materials* **192**, p. 874-879 (2011)
- [2]. X. Zhang, H. Tao, Z. Zhang, J. Liu, X. Liu, *Applied Thermal Engineering* **132**, p. 801-807 (2018)
- [3]. M. Gomez-Mares, M. Zarate, J. Casal, *Fire Safety Journal* **43(8)**, p. 583-588 (2009)
- [4]. N. Gopalaswami, Y. Liu, D.M. Laboureur, B. Zhang, M. Sam Mannan, *Journal of Loss Prevention in the Process Industries* **41**, p. 365-375 (2016)
- [5]. C. Tao, Y. Shen, R. Zong, *Applied Thermal Engineering* **91**, p. 884-887 (2016)
- [6]. D.M. Laboureur, N. Gopalaswami, Y. Liu, B. Zhang, M. Sam Mannan, *Journal of Loss Prevention in the Process Industries* **41**, p. 355-364 (2016)
- [7]. B. Zhang, Y. Liu, D. Laboureur, D. Mannan, *Ind. Chem. Res.* **54 (37)**, p. 9251-9256 (2015)
- [8]. P.S. Cumber, M. Spearpoint, *Fire Safety Journal* **41 (3)**, p. 215-228 (2006)
- [9]. X.L. Zhang, L.H. Hu, Q. Wang, X.C. Zhang, Y. Jiang, *Applied Thermal Engineering* **110**, p. 11-114 (2017)
- [11]. I.W. Ekoto, A.J. Ruggles, L.W. Creitz, J.X. Li, *Int. J. Hydrogen Energy* **39**, p. 20570-20577 (2014)
- [12]. K. Zhou, J. Liu, J. Jiang, *Applied Thermal Engineering* **106**, p. 634-639 (2016)
- [13]. K. Zhou, J. Jiang, *J. Heat Transfer* **138** (2015)
- [14]. M. Gomez-Mares, M. Munoz, J. Casal, *Axial temperature distribution in vertical jet fires*, *J. of Hazardous Materials*, **172**, p. 54-60 (2009)
- [15]. X. Zhang, L. Hu, W. Zhu, X. Zhang, L. Yang, *Applied Thermal Engineering* **73**, p. 15-22 (2014)
- [16]. A. Palacios, M. Munoz, R.M. Darbra, J. Casal, *Fire Safety Journal* **51**, p. 93-101 (2012)
- [17]. A. Palacios, J. Casal, *Fuel* **90**, p. 824-833 (2011)
- [18]. L. Hu, Q. Wang, F. Tang, M. Delichatsios, X. Zhang, *Fuel* **106**, p. 779-786 (2013)
- [19]. M. Gomez-Mares, M. Munoz, J. Casal, *Experimental Thermal and Fluid Science* **34**, p. 323-329 (2010)
- [20]. D.Y. Krian, D.P. Mishra, *Fuel* **86**, p. 1545-1551 (2007)
- [21]. S.R. Gollahalli, T.A. Brzustowski, H.F. Sullivan, *Transactions to the CSME 1975*, **3(4)**, p. 205-214 (1975)
- [22]. Y. A. Cengel, *Heat and Mass Transfer*, McGraw Hill (2006)
- [23]. H. Clewell, Energy Systems Laboratory, ESLTR-83-03, (1983)
- [24]. P. Cumber, *Journal of Hazardous Materials*, **A89** (2002)
- [25]. *Guidelines for Evaluating the Characteristics of Vapor Cloud Explosions, Flash Fires and BLEVE's* (American Institute of Chemical Engineers, 1994)
- [26]. J. P. Holman, *Heat transfer* (McGraw Hill, 1992)
- [27]. D. Incropera, L. Bergman, *Fundamentals of Heat and Mass Transfer* (Willey, 2006)
- [28]. A. F. Mills, *Heat Transfer* (Prentice Hall, 1998)
- [29]. R. H. Perry and D. W. Green, *Perry's Chemical Engineers' Handbook* (The McGraw-Hill Companies, 1999)
- [30]. P. K. Ramskill, *The development of ENGULF to model a multi-component liquid in a fire engulfed tank* (UKAEA Safety and Reliability Directorate, 1987)